Journal of
Materials Chemistry B

Accepted Manuscript

This is an *Accepted Manuscript*, which has been through the RSC Publishing peer review process and has been accepted for publication.

Accepted Manuscripts are published online shortly after acceptance, which is prior to technical editing, formatting and proof reading. This free service from RSC Publishing allows authors to make their results available to the community, in citable form, before publication of the edited article. This *Accepted Manuscript* will be replaced by the edited and formatted *Advance Article* as soon as this is available.

To cite this manuscript please use its permanent Digital Object Identifier (DOI®), which is identical for all formats of publication.

More information about *Accepted Manuscripts* can be found in the **Information for Authors**.

Please note that technical editing may introduce minor changes to the text and/or graphics contained in the manuscript submitted by the author(s) which may alter content, and that the standard **Terms & Conditions** and the **ethical guidelines** that apply to the journal are still applicable. In no event shall the RSC be held responsible for any errors or omissions in these *Accepted Manuscript* manuscripts or any consequences arising from the use of any information contained in them.

The table of contents entry

Structural analogy with antibacterial peptides provides antibacterial property in newly developed HAp/Au/arginine nanocomposite. The material possesses: (i) high antibacterial activity, (ii) high cytocompatibility and (iii) good stability in physiological environment.

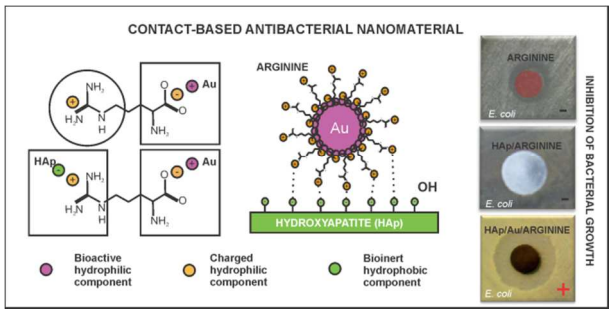

Journal of Materials Chemistry B

RSCPublishing

ARTICLE

Hydroxyapatite/Gold/Arginine: Designing the Structure to Create Antibacterial Activity

Cite this: DOI: 10.1039/x0xx00000x

M. Vukomanović,[a,*] M. Logar,[a,b] S. D. Škapin,[a] and D. Suvorov,[a]

Received 00th January 2012,
Accepted 00th January 2012

DOI: 10.1039/x0xx00000x

www.rsc.org/

Antimicrobial peptides, selective antimicrobials able to "recognize" and "target" bacterial cells, are significant advancement in comparison to non-selective antimicrobials widely used in practice. The major problem of this class of macromolecules is, however, a short half-life. Starting from the key physicochemical properties of antibacterial peptides, our intention was to develop their stable analogue. We designed hydroxyapatite/gold/arginine (HAp/Au/arginine) nanocomposite that contains: (i) hydrophobic gold (Au) nanoparticles, (b) positively charged, hydrophilic arginine molecules that functionalize the surface of the Au and (c) hydroxyapatite (HAp) bioactive carrier of the functionalized Au nanoparticles. None of the components used for the formation of the nanocomposite have any influence on bacterial growth; however, its structure with specific chemistry of the surface, which is analogous to that of antibacterial peptides, provides this property. The developed nanocomposite possesses all the beneficial properties of antibacterial peptides and is one step ahead of them as far as stability is concerned. The material follows contact-based mechanism significantly improved in comparison to metabolism-involved mechanism of antibacterial peptides. In comparison to the non-selective HAp/Ag reference, newly-developed material possesses stronger antibacterial action, is more compatible to human cells and can be suggested as safer and more effective replacement of Ag-based antibacterial components in biomaterials.

Introduction

Silver-based nanomaterials are one of the most frequently used option for ensuring the antimicrobial function in biomaterials.[1] The major problem in this class of antimicrobials is in their non-selectivity expressed through the same way of action with human and bacterial cells. Comparison of the toxicity induced by Ag and Au nanoparticle tested in zebra-fish model confirmed 100% mortality induced by Ag nanoparticles in about 120 hours, while Au nanoparticles induced less than 3% mortality for the same period of time.[2] However, in comparison to Ag with natural antimicrobial activity, in Au nanoparticles this property needs to be designed.

A promising direction for the future development of novel tools that are able to prevent and stop microbial infections as well as to prevent further competition with the capacity of bacteria to develop a novel route to resistance [2-8] is in the design of innovative, non-conventional antimicrobials. The paradigm of "nano-antibiotics" offers a huge potential.[9] The versatility of the methods [9-11] able to control the shape, size and surface of the nanoparticles as well as to develop a "smart" mechanism that allows them to "recognize" a specific environment and to "target" a pre-defined action after "sensing" the targeting object provides a lot of space to design advanced antimicrobials.

The core-shell nanostructures, formed of lysosome-coated silica nanoparticles, are developed as very potent antimicrobial activity obtained both *in vitro* and *in vivo* with low cytotoxicity and negligible haemolytic side effect. It has been suggested that tailoring these nanostructures will find their special application in action against bacteria especially when challenge of the increasing severity of multidrug resistance is concerned.[12]

Formation of core-shell structures of self-assembled cationic antibacterial peptides is the next significant step forward in developing nano-antibiotics that are able to target bacteria.[13] Antibacterial peptides, in general, are made of a specific sequence of amino acid residues containing a few charged hydrophilic amino acids, with the rest being hydrophobic. The amphipathicity of these molecules enables them to cross the membrane and interact with both the hydrophobic and hydrophilic components of the membrane lipid bilayer. The main mechanism of their action is based on electrostatic interactions. The amino acid- residues with charged groups (usually arginine and/or lysine) [14,15] interact with the surface of the bacterial cellular walls and disrupt their structure. Usually, they form a pore within the bacterial wall or change its permeability, which allows them to transfer across all the barriers and makes it possible to enter the interior of the bacterial cell. Inside the cell they affect the intercellular compartments or they are involved in some essential functions such as protein synthesis, membrane synthesis, nucleic acid structure, etc.[16] Therefore, these peptides follow an antibacterial mechanism based on the surface charge to "sense" the bacterial surface, to damage it and/or to cross it and get inside the cell, where they target various metabolic pathways that are essential for their life. It was not easy for the bacteria to develop a resistance mechanism for this multi-targeting mechanism of

antibacterial action. Therefore, this class of antimicrobials has proven to be very effective against multi-drug-resistant microbes.[14,15] The main drawback that limits the practical application of this group of antimicrobials is its instability and short half-life induced by the enzymatic degradation and inactivation by the host binding proteins, the limited targeting due to the expulsion by multi -drug pumps and the alternation of the membrane fluidity.[17,18] The impressive advantages and major disadvantages of antibacterial peptide were our motivation for the development of an innovative design of antibacterial nanomaterial. Gold is a bio-inert metal that is compatible with living surroundings, without any ability for antibacterial action. Some bacteria even have the ability to uptake Au -compounds, reduce them and excrete in the form of pure, metallic Au nanoparticles.[19] Recently, different methods for the bio-activation of this metal have been developed, which opened many branches for its application in biomedicine.[20] The most promising among them concern the use of Au nanoparticles as the carriers of drugs (like antibiotics),[21] as diagnostics (as contrasting agents)[22] and as therapeutics (for photo-thermal therapy).[23] Such an approach introduced Au as a novel biomaterial and opened a new chapter in biomaterial design. We used hydrophobic Au as a building component to design a novel, stable analogous to antibacterial peptides with the structure carefully developed within a HAp/Au/arginine nanocomposite. The basic idea was to form non-degradable analogues of the antibacterial peptides as stable, safe and effective replacement of Ag-based antimicrobials. For this purpose we developed HAp/Au nanoparticles and functionalized them with arginine (using novel, recently patented technology).[24] Our research came from the hypothesis that joining the following properties mimicked from antibacterial peptides such as (i) hydro-phobic/hydrophilic segments, (ii) a cationic, charged surface and (iii) non-degradable and slowly bioresorbable components, will provide a way to design a very efficient, antibacterial property in the resulting nanocomposite.

Experimental

Synthesis of HAp/Au/arginine

The affinity of gold surface to bond amines was used for the development of the sonochemical method for the synthesis of HAp/Au functionalized by arginine.[24] HAp (c=1.5 $mg \cdot ml^{-1}$) previously synthesized using sonochemical homogeneous precipitation was re-dispersed into an isopropanol solution in water (c=$2 \cdot 10^{-2}$ $ml \cdot ml^{-1}$) using ultrasonication (time of sonication t=10 min., pulsation-to-relaxation periods on:off=02:01, T=25°C, power P=600W, frequency f=20 kHz and amplitude A=80%). After the dispersion period was finished, a water solution of chloroauric acid ($HAuCl_4$) (c=0.8 $mg \cdot ml^{-1}$, 50 ml) and arginine (n($HAuCl_4$) : n(arginine) = 1 : 1 mol/mol, 50 ml) were added and sonificated for an additional 30 min. The obtained precipitates were separated from supernatant by centrifugation (15 min. at 5000 rpm) and air-dried on glass slides. All the experiments were performed using an Ultrasonic Processor for High Volume Applications VCX 750, Newtown, Connecticut, USA.

Physicochemical properties investigations

XRD analyses were performed using a Bruker AXS D4 Endeavor diffractometer and the samples were recorded in the 2θ range from 2° to 70° with a step size of 0.02° and a time of 2 $s \cdot step^{-1}$. Elemental composition analyses of the surface were carried out on the PHI-TFA XPS spectrometer which excites the sample's surface by X-ray radiation from an Al-monochromatic source. The survey and narrow scan spectra of the emitted photoelectrons were taken with 187 eV and 29 eV. The data were treated with the Multipak program, Version 8.1. The sensitivity of the applied method is up to 0.05 at.%. All the data were obtained by averaging at least three repeated integrations of the peaks. The optical properties were analysed based on absorption spectra measured on a UV-VIS-NIR spectrophotometer (Shimadzu UV-3600) in the range between 200 and 800 nm with a spectral resolution of 0.1 nm. Scanning transmission electron microscopy (STEM) was employed to investigate the morphology and structural characteristics of the HAp/Au composite. The sample was dispersed in deionized water and drop casted onto a lacey carbon TEM grid for the TEM characterization. TEM imaging, energy-dispersive X-ray spectroscopy (EDX) mapping and EEL spectra acquisition in the scanning transmission electron microscopy (STEM) mode were performed in a FEI Titan Scanning Transmission Electron Microscope (STEM) operating at 300 kV, equipped with a Cs image corrector and a monochromator operated at 300 kV. The TEM images were taken using an Ultrascan 1000 CCD camera at binning 2 (1024 × 1024 pixels) and an exposure time of 0.5 s per image. The EEL spectra were acquired in the monochromated TEM imaging mode, using a Gatan Tridiem 866 EEL spectrometer with a 2.5 -mm entrance aperture. The dispersion setting was 0.01 $eV \cdot pixel^{-1}$, and the energy resolution for these experiments (defined by the fwhm of the zero loss peak) was 0.12 eV. The convergence semi-angle was 9.6 mrad and the collection semi-angle was 16. The spectra were acquired with Titan imaging and Analysis (TIA) software by directing the electron beam onto the edge of the Au nanoparticles attached to the HAp with an acquisition time of 50 ms. The EELs data were post processed in Digital micrograph. To reveal the surface plasmon resonance (SPR) of the Au nanoparticles the zero-loss peak was first fitted to the sum of the Gaussian and Lorenzian curves and subsequently subtracted from the spectra.

In vitro antibacterial tests

The 8 -mm of tested materials were put on the surface of the agar plates with *E. coli* (K-12 MG1655) and *S. aureus* collected during the log phase, turned upside down and incubated at 37 °C for the next 24 h. The zones of the inhibition of bacteria growth were photographed as well as observed with an optical microscope (Olympus BX series) using a phase-contrast technique. The test was performed in two parallel series.
The detection of dead and live *E. coli* and *S. aureus* as well as their distribution on the surface of the disks and within the zone of inhibition were tested after staining using Live/Dead BacLight Bacterial Viability Kit (Molecular Probes, Inc.) consisting of two fluorescent dyes, i.e., SYTO 9 and propidium iodide (PI), and investigated using fluorescence microscopy (Olympus IX81 inverted research microscope). The examinations were performed in two parallel series of investigated composites.
The morphological and structural properties of the *E. coli* and *S. aureus* were performed for bacteria selected from the inhibition zone near the surface of the disks made of tested material, while bacteria growing in the healthy colony far from the disc were used as the negative controls. The bacteria were fixed in 1% formaldehyde and 0.5% glutaraldehyde in a 0.1-M phosphate buffer solution (pH = 7.4) at 4°C, post-fixed using a

1% aqueous solution of osmium-tetroxide for 1 hour, dehydrated in 50%, 70%, 90% and 100% ethanol solutions and finally in 100% acetone and dried using the critical -point drying method in a CPD030 dryer (Balzers). Before the SEM examination the samples were coated with platinum in a sputter -coater SCD 050 (BAL-TEC).

In vitro stability investigations

The stability was investigated by incubating the nanocomposite under pH = 7.4, 5.4 or 3.4 using a PBS buffer (Sigma Aldrich, Germany) with the acidity maintained by HCl (Sigma Aldrich, Germany) at 37°C and a 60-rpm shaking rate. The total release of the metallic ions and the phase composition of the remaining powders were investigated over a period of ten days using the inductively coupled plasma atomic emission spectrometric (ICP AES) (Thermo Jarrell Ash, model Atomscan 25) method and above -described XRD method, respectively. The investigation was performed with two parallel measurements.

In vitro citocompatibility tests

In vitro citocompatibility tests: The *in vitro* cytotoxicity tests were performed on human foetal lung fibroblasts (IMR-90) (ECCAC no. 85020204) and human osteosarcoma (U-2 OS) (ECCAC no. 92022711) cell lines. To analyse the cell viability after exposure to the materials the cells were plated in 24-well plates, at least one day before the treatment. The tested materials were dispersed in a culture media and added to the cell cultures at different concentrations. After 24 hours of exposure to the materials the cells were trypsinized and stained with annexin V (BD Biosciences, Pharmingen, San Diego/CA, USA) and propidium iodide (Sigma-Aldrich; St. Louis/MO, USA). The samples were than analysed using a FASCalibur flow cytometer (BD; Franklin Lakes/NJ, USA) and the CellQuestTM software, Version 3.3 (FACSComp Software, BD; Franklin Lakes/NJ, USA). The acquisition was stopped when at least 5000 events were acquired in the cell region and the percentages of viable cells (annexin V and PI double negative) were determined. Two independent experiments were performed in duplicates.

Results and discussion

The structure of HAp/Au functionalized with arginine

In order to obtain a HAp/Au nanocomposite with a functionalized surface a novel method based on the sonochemical approach has been developed. Sonification of a water/isopropanol solution of arginine allows the formation of reactive radicals that are able to reduce the HAuCl4 used as an Au -precursor. The procedure provides a single crystalline phase that corresponds to the structure of cubic Au (JCPDS No.: 4-0784) (Fig. 1a). In the case when the solution of the Au -precursor contains dispersed HAp particles, the reduction of the Au during sonification leads to the formation of the HAp/Au nanocomposite with cubic Au (JCPDS No.: 4-0784) and hexagonal HAp (JCPDS No.: 9-0432) (Fig. 1b).
During the formation of the nanocomposite, besides the reduction of the Au -precursor the arginine remains attached on the formed Au -nanoparticles and provides functionalization. The N1s region of the XPS spectrum of the HAp/Au nanocomposite reveals two superimposed singlets at 398.7 eV and 400.2 eV (Fig. 1c). The first one indicates amino -groups bonded by a chemisorption process, while the second indicates free amines physisorbed at the metallic surface.[25] These components were assigned to amines chemically adsorbed on the Au nanoparticles as well as to free amines and amines physically adsorbed at the HAp template.

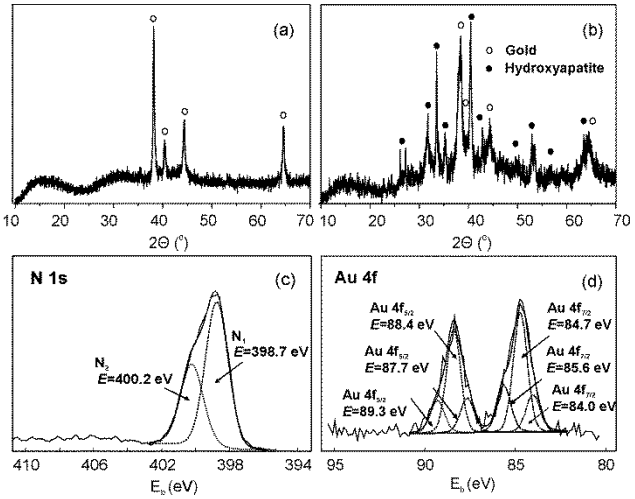

Fig. 1 Phase composition and surface chemistry of HAp/Au/arginine. XRD patters of Au nanoparticles (a) and HAp/Au/arginine nanocomposite (b) with deconvoluted N1s XPS spectra of the HAp/Au/arginine (c) corresponding to the arginine molecules attached to the surface of Au nanoparticles and Au4f XPS spectra of the HAp/Au/arginine (d) corresponding to the functionalized Au nanoparticles attached to HAp plates.

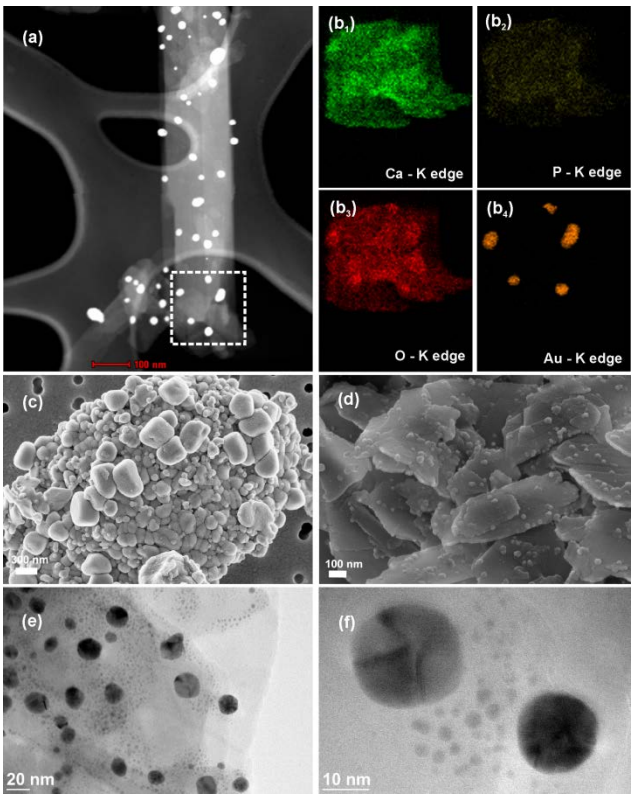

Fig. 2 Morphological and structural properties of HAp/Au/arginine. Dark -field STEM micrographs and EDX mapping of the nanocomposite showing corresponding Ca, P, O and Au elemental maps (a, b_{1-4}). SEM micrograph of Au/arginine without and with templating influence of HAp (e,d) and TEM images showing the size, shape and distribution of Au/arginine attached onto the HAp plates (e,f).

An Au4f spectrum of HAp/Au contains a doublet with wide (fwhm = 2.0 eV), non-symmetric peaks with three components (Fig. 1d): (i) first low-intensity doublet (84.0 and 87.7 eV) that corresponds to the Au(0) templated by HAp, (ii) second low-intensity doublet (85.6 and 89.3 eV) that belongs to the oxidized surface-complexing Au(+1) and indicates the presence of the surface layer of oxidized Au involved in the functionalization process and (iii) third, the most intensive Au doublet (84.7 and 88.4 eV) that corresponds to the pure elemental gold (like for the polycrystalline Au reference) that belongs to the core of the surface-functionalized Au nanoparticles.[26] The so-formed functionalized Au nanoparticles are uniformly distributed along the surface of the HAp plate (Fig. 2a). Calcium, phosphorus and oxygen elemental maps (Fig. $2b_{1-3}$) identified the HAp template phase, while the gold map (Fig. $2b_4$) confirmed the formation of the Au nanoparticles present at its surface. In the absence of the HAp template, the Au particles have an irregular morphology, forming highly agglomerated spheres up to 500 nm in diameter (Fig. 2c). Within the HAp/Au, the Au nanoparticles are spheres with an average size of 9.2±5.5 nm. The HAp component significantly affects the growth characteristics of these particles, allows their stabilization and prevents any agglomeration and ingrowths into larger structures (Fig. 2d-f).

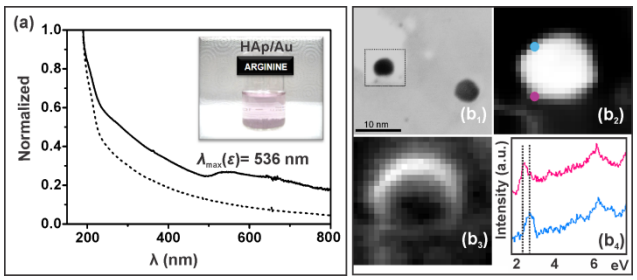

Fig. 3 Surface plasmon resonance of HAp/Au/arginine. UV/Vis spectra of HAp (dotted line) and its nanocomposite with Au/arginine (solid line) with the inset photograph of the water dispersion of the HAp/Au/arginine nanocomposite. Selected 10-nm Au nanoparticle (b1) and the associated EEL spectra (b2-4) corresponding to the LSPR of the selected Au nanoparticles within the nanocomposite.

A contact between HAp template and Au nanoparticles at their surface was investigated based on the optical properties of the nanocomposite. The water dispersion of HAp/Au/arginine shows a light -violet colour (inset in Fig. 3a). Its UV/Vis absorption spectrum (Fig. 3a) has the broad absorption of the HAp super-imposed on the absorption of the Au nanoparticles with a maximum at 536 nm (2.30 eV). The SPR maximum has a significant red-shift in comparison to the SPR maximum of the isolated Au nanoparticles of comparable size, which appears at 520 nm (2.38 eV).[27] The change in the SPR maximum is simultaneously assigned to the higher permittivity of the surrounding, contacting HAp plate and the surface functionalization of the Au nanoparticles in the as -formed HAp/Au nanocomposite.

Along with the classic, spectroscopic investigations, EELS was employed to investigate the plasmonic properties of as -formed HAp/Au nanocomposite. The procedure based on using a monochromated electron beam in STEM mode[28] has been applied. A 10-nm Au nanoparticle attached to the surface of the HAp was selected and investigated in terms of the local SPR (Fig. $3b_1$). The pink dot in Fig. $3b_2$ indicates the excited position at the surface of the Au/arginine nanoparticle on the edge close to the surface of the HAp, while the blue one indicates the excited position on contact-free edge of the Au/arginine nanoparticles. The EELs map in the energy interval between 2.45 eV and 2.55 eV (Fig. $3b_3$) reflects the SPR of the Au/arginine nanoparticle. The excitation of these positions using an electron beam results in EEL spectral peaks in the low -loss region that corresponds to the particle's LSPR. The SPR spectral peak obtained by exciting the Au edge in contact with the HAp exhibits a red shift in comparison to the SPR peak obtained by exciting the free edge of the Au nanoparticles (Fig. $3b_4$), which is induced by an increased dielectric constant of the Au nanoparticle surrounding at the junction with the HAp plate. Both investigations showed the existence of interactions between the HAp surface and the surface of the functionalized Au nanoparticles, confirming their stabilization by attachment onto the HAp plates within the HAp/Au/arginine nanocomposite.

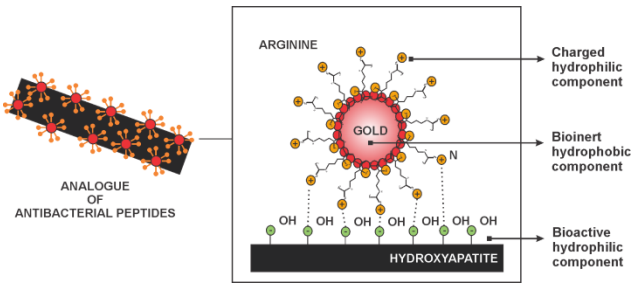

Fig. 4 The structure of HAp/Au/arginine. Schematic illustration of the structural properties of the nanocomposite as analogue of antibacterial peptides that contains hydrophobic Au with the surface functionalized by charged, arginine molecules attached onto the surface of bioactive HAp plates.

Based on the investigated physicochemical properties we came to the conclusion that developed HAp/Au/arginine nanocomposite contains three major components: (i) a hydrophilic, charged amino acid, (ii) hydrophobic, bioinert Au nanoparticles and (iii) a hydrophilic, bioactive HAp with the structure illustrated in Fig. 4. The structure of the nanocomposite contains Au nanoparticles with arginine molecules covalently bonded to their surface. The bonding is obtained between the surface Au atoms and the amino groups of the arginine molecules with free, charged guanidinium groups at the opposite side. The functionalized Au nanoparticles are uniformly distributed and attached onto the surface of the HAp that uses electrostatic interactions to template them and prevent their further growth.

Antibacterial properties of HAp/Au functionalized with arginine

In order to prove the concept, the susceptibilities of *E. coli* (Fig. $5a_{1-3}$) and *S. aureus* (Fig. $5a_{4-6}$) were investigated for three parallel series containing: (i) arginine, (ii) HAp/arginine and (iii) HAp/Au/arginine. The arginine was compacted into a disc containing 100% of amino acid (indicated by the red circle in Fig. $5a_1$,a_4) that was incubated with bacteria. After aging in agar media, the disc was completely dissolved and the whole quantity of amino acid diffused into the surrounding area. Even though a large quantity of arginine diffused, it was not able to inhibit the bacterial growth, confirming its inability for antibacterial activity. Similarly, during testing the HAp/arginine (Fig. $5a_2$,a_5) the bacteria were able to grow close to the surface of the discs and below them, confirming the absence of the antibacterial activity. The only case when the susceptibilities of both investigated bacteria were confirmed was when testing the

HAp/Au/arginine nanocomposite. The appearance of the ring around the disc made of HAp/Au/arginine (Fig. 5a_3,a_6) indicated the formation of the zones of bacterial growth and confirmed the antibacterial activity of the nanocomposite. Concerning the inability of arginine and HAp/arginine to act against bacteria, the antibacterial activity of the HAp/Au/arginine nanocomposite is assigned to the joint activity of all three components within a special structure of the newly developed nanocomposite.

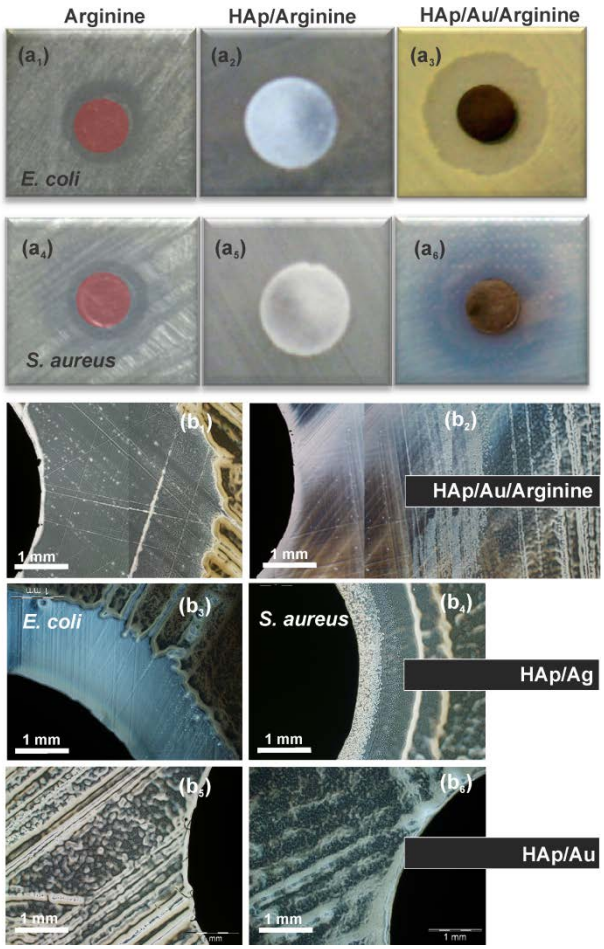

Fig. 5 Bacterial susceptibility tests. Disk diffusion analysis of *E. coli* and *S. aureus* for arginine (a_1, a_4), HAp/arginine (a_2, a_5) and HAp/Au/arginine (a_3, a_6). Comparison of the zones of inhibition of *E. coli* and *S. aureus* bacterial growth induced by HAp/Au/arginine (b_1,b_2) HAp/Ag (b_3,b_4) and HAp/Au without functionalization (b_5,b_6).

The zones of inhibition of bacterial growth induced by the HAp/Au/arginine were compared to the zones of inhibition induced by the HAp/Ag, with 10 wt% of silver as well-known antibacterial agent. The HAp/Ag nanocomposite, used as a positive control for inhibition of bacterial growth, was formed by sonochemical synthesis followed by thermal reduction (as described elsewhere[29]). So-obtained Ag nanoparticles were formed without any functionalization of the surface and obtained antibacterial activity is solely a consequence of natural ability of Ag for action against bacteria. The HAp/Au/arginine inhibited growth of *E. coli* with-in two -times larger zone around the disc in comparison to HAp/Ag (Fig. 5b_1,b_3) confirming stronger antibacterial action. Similar was obtained for the *S. aureus*. A larger zone of inhibition of bacterial growth induced by HAp/Au/arginine confirmed stronger susceptibility of *S. aureus* to HAp/Au/arginine than to HAp/Ag nanocomposite (Fig. 5b_2,b_4). In comparison to them and similar to the pure HAp, HAp/Au nanocomposite without functionalization (obtained by thermal reduction in accordance to the procedure described elsewhere[29]) did not showed any influence to bacterial growth (Fig. 5b_5,b_6).

To distinguish between the viable and death cells, bacteria selected from the zone of inhibition of bacterial growth were stained in situ using SYTO 9 and PI fluorescence dyes. The SYTO 9 is a cell -membrane-permeable green fluorescent dye that binds to nucleic acids of both dead and viable cells, while PI is a red fluorescence dye that is impermeable to intact membranes, penetrates only mechanically destroyed or damaged membranes and binds to the nucleic acids of dead bacteria.[30] Staining the region far from the HAp/Au/arginine disc, outside of the zone of inhibition of bacterial growth, revealed a large population of viable cells for both *E. coli* and *S. aureus* (Fig. 6a_1,a3). In contrast, in the region within the zone of inhibition of bacterial growth, close to the surface of the disc, the grown population was poor and the majority of the bacteria were stained by the red PI fluorescent dye, indicating dead cells for both *E. coli* and *S. aureus* (Fig. 6a_2,a_4).

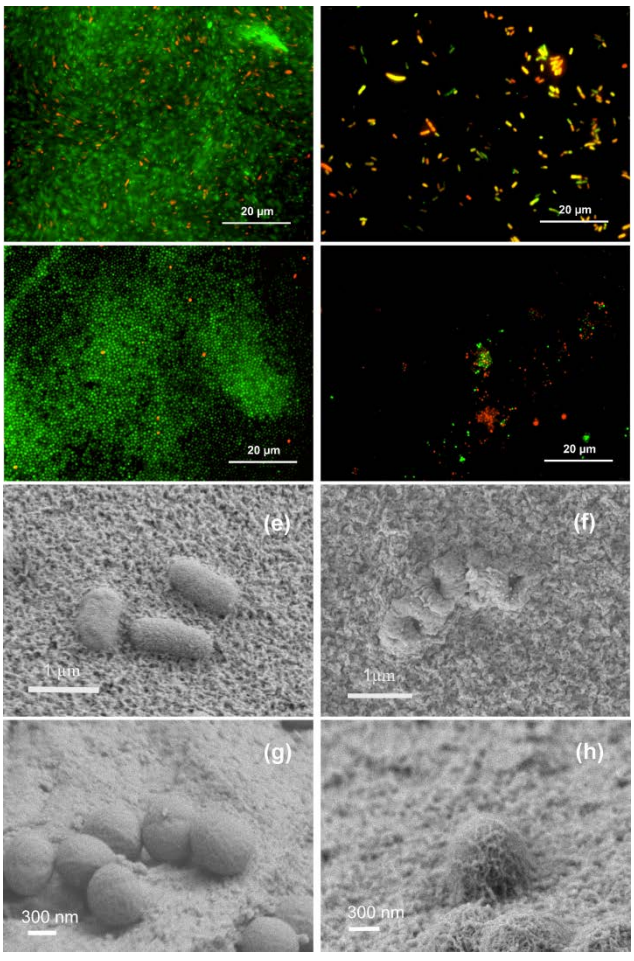

Fig. 6 Morphology of dead/live bacteria. SYTO/PI dead/live test for *E. coli* and *S. aureus* in the case of intact bacteria (a_1, a_3) and bacteria incubated with HAp/Au/arginine (a_2, a_4). SEM analysis for *E. coli* and *S. aureus* of intact bacteria (b_1, b_3) and bacteria incubated with HAp/Au/arginine (b_2, b_4).

Distinguished dead and intact bacteria were selected for further morphological investigations to reveal the way of damaging induced by HAp/Au/arginine. The intact *E. coli* bacteria were

1μm-long rod-like cells (Fig. 6b$_1$). In comparison to them, the bacteria selected from the region of the zone of inhibition of bacterial growth had an obvious cellular disruption. They were wrapped into coils, shrunken and with a folded surface of the outer membrane (Fig. 6b$_2$) (for more details please see DOI: 10.1039/b000000x/). These changes indicate a loss of integrity of the membrane, most probably because of structural changes in the peptidoglycan layer. In comparison to the intact *S. aureus* bacterial cell which are sphere-like in shape, with diameters between 200 and 500 nm, and a smooth surface (Fig. 6b$_3$), the bacteria selected from the region close to the surface of the HAp/Au/arginine did not undergo obvious changes in the structural integrity of the cell. However, the change of the roughness of their surface was detected since they were coated with a filamentous network (Fig. 6b$_4$). This surface layer can be attributed to the protein, mucosa layer that participates in the formation of biofilms and has a protective role in the Gram - positive bacteria.[31]

In vitro stability and cytocompatibility of HAp/Au functionalized with arginine

The *in vitro* properties of the HAp/Au/arginine nanocomposite were investigated starting from the ability to release metallic ions and to change phase composition. After the incubation of the nanocomposite under *in vitro* conditions for a period of 10 days it has the capacity to release less than 0.007 mg/ml of Au - ions (Fig. 7a). Within the tested range of pH, which was from 3.4 to 7.4, its solubility and ability to release metallic ions are independent of the acidity showing very similar concentrations. The powders obtained after *in vitro* incubation were also investigated for phase composition and the same phases as the starting nanocomposite has been confirmed (Fig. 7b). The detected NaCl belongs to the PBS buffer, and it remained within the material from the medium after drying the powders. The formation of any additional phase containing gold, calcium or phosphates was not detected. The same phase composition was obtained for the whole pH range, starting from 3.4 to 7.4. Such chemical and phase stability of the nanocomposite is attributed to the low chemical reactivity of the gold. This stability indicates that the previously observed antibacterial activity of the HAp/Au/arginine nanocomposite follows a contact-based mechanism and is independent of the dissolution and release of metallic ions. It has been already shown that other materials including chitosan and its derivatives follow contact-based mechanism and have a property to use surface charge to interact with negatively charged bacterial surface. This mechanism offers numerous benefits to medical applications including long-lasting antibacterial activity and significantly reduced chances for development of bacterial resistivity.[32,33] Chemical stability of HAp/Au/arginine under *in vitro* conditions also suggests the possibility for a high level of compatibility of this nanocomposite with human cells.

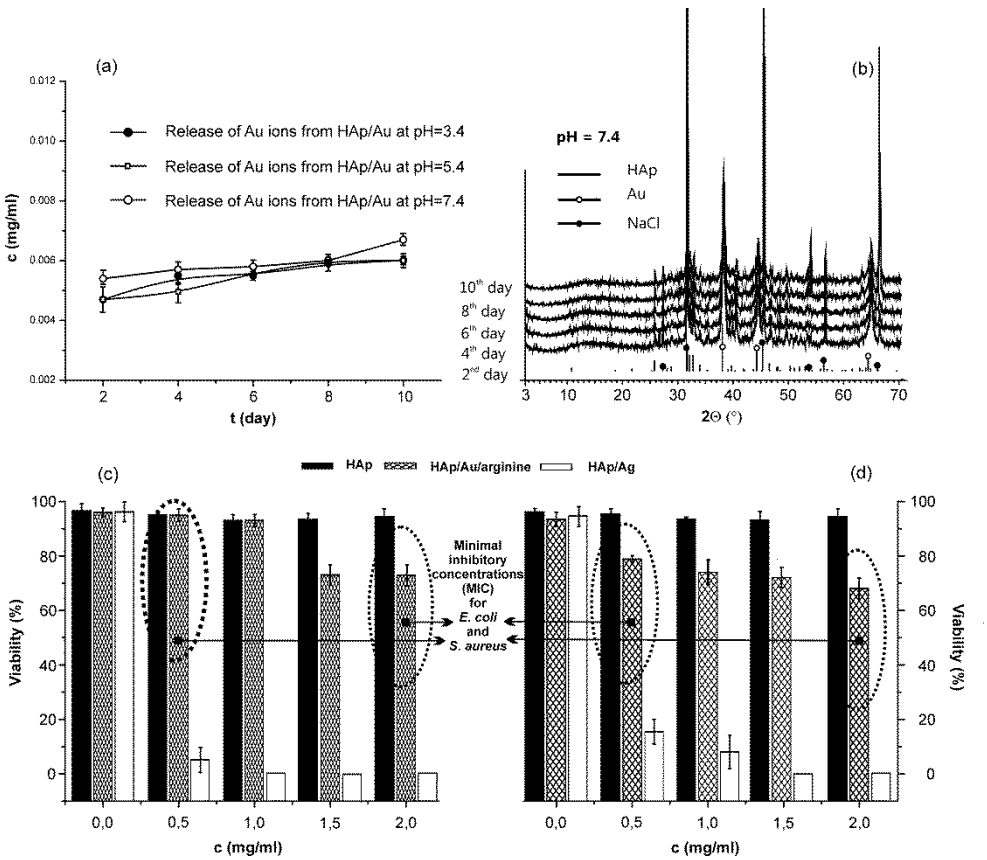

Fig. 7 *In vitro* stability and cytocompatibility of HAp/Au/arginine. Release of metallic ions within incubation media (a) and phase composition of the remained powder (b) obtained after incubation of the HAp/Au/arginine during a 10-days period. Viability of IMR-90 human fetal lung fibroblasts (c) and U-2 human osteosarcoma cells (d) after 24-hour of incubation with different concentrations of HAp, HAp/Ag and HAp/Au/arginine.

The cytocompatibility of the HAp/Au functionalized with arginine was tested in U-2 human osteosarcoma and IMR-90 human foetal lung fibroblast cells (Fig. 7c,d). The results were compared to HAp, which is known as a highly bioactive

biomaterial that was used as negative probe, and to HAp/Ag, which contains toxic silver, used as a positive probe. As expected, after incubation with HAp, a very high percentage of viability was obtained for both types of investigated cells. The viability was high for the whole range of tested concentrations up to 2 mg/ml. In contrast, incubation with HAp/Ag provided a rapid decrease of the percentage of viable cells. Even for the concentrations that were about 0.5 mg/ml, the viability of the IMR-90 was less than 10% and the viability of the U-2 OS was less than 20%, indicating the very high toxicity of the HAp/Ag nanocomposite. When the HAp/Au/arginine was tested, the lowest level of viability was 70%, and this was obtained for a concentration of 2 mg/ml of the nanocomposite. At the minimum concentration of HAp/Au/arginine that inhibits the growth of *E. coli* (MIC for *E. coli*) the viabilities of the IMR-90 and U-2 OS were more than 90% and 80%, respectively. Similarly, at a concentration that inhibits the growth of *S. aureus* (MIC for *S. aureus*) the viabilities of the IMR-90 and U-2 OS were more than 70%. These results indicate that, in contrast to the antibacterial HAp/Ag that uses the same mechanism for interaction with both human and bacterial cells applying general toxicity as the main mechanism of antibacterial action, HAp/Au/arginine is selective and has the possibility to interact with human and bacterial cells in a different manner that includes using the specific structure and specially designed surface chemistry to recognize bacterial cells and target them.

A comparison between antibacterial peptides and the HAp/Au/arginine shows a significant similarity, starting from a similar structure that leads to a similar way of interaction with cells. In HAp/Au/arginine there are hydrophobic/hydrophilic segments, a cationic, charged surface and non-degradable, slowly resorbable components. A positively charged guanidine group with the charge delocalized among all three amines allows very good selectivity with a much higher affinity for an interaction with the strongly negative surface of bacteria, compared to the less negative or positive surface of mammalian cells. Consequently, it provides the possibility to join effective antibacterial with good biocompatibility properties within a single HAp/Au/arginine nanocomposite. In the same time, the main differences between antibacterial peptides and HAp/Au/arginine that include lower reactivity, higher selectivity and significantly improved stability of the nanocomposite are the major benefits of this newly developed antibacterial biomaterial. With these properties it presents a perspective approach in the design of antibacterial property in biomaterials and opens up a novel direction in searching for effective and safe antibacterial protection with full capacity to replace toxic Ag-based antimicrobials.

Conclusions

Based on the analogy with natural-sourced antibacterial peptides, we design very efficient antibacterial property in a novel HAp/Au/arginine nanocomposite. We also confirmed a possibility to create antibacterial property in a material by specific tuning of its structure and chemistry of the surface mimicking natural-sourced model. The so-developed nanocomposite binds three significant properties: (i) a high antibacterial activity, (ii) a high cytocompatibility with human cells and (iii) stability in a physiological environment. These properties classify the newly developed nanocomposite as highly perspective for biomedical applications as an antibacterial nanocomposite able to provide the safe and efficient prevention and treatment of infection. It has the capacity to replace currently used toxic antibacterial components such as silver and provides an innovative direction for research in novel nonconventional antibacterial agents highly applicable in the field of biomedicine.

Acknowledgements

The authors are grateful to Assist. Prof. Dr. Tina Zavašnik-Bergant and Dr. Urška Repnik from the Department for Biochemistry and Molecular and Structural Biology at the Jožef Stefan Institute for the antibacterial and cytocompatibility tests.

Notes and references

[a] Advanced Materials Department, Jožef Stefan Institute, Jamova 39, 1000 Ljubljana, Slovenia; tel.: +386 1 477 3547; e-mail: marija.vukomanovic@ijs.si

[b] Department of Materials Science and Engineering, Stanford University, Lomita Mall 496, California.

Electronic Supplementary Information (ESI) available: SEM images showing more detailed information regarding morphological characteristics of *E. coli* after exposure to HAp/Au/arginine. See DOI: 10.1039/b000000x/

1 S. W. P. Wijnhoven, W. J. G. M. Peijnenburg, C. A. Herberts, W. I. Hagens, A. G. Oomen, E. H. W. Heugens, B. Roszek, J. Bisschops, I. Gosens, D. V. D. Meent, S. Dekkers, W. H. D. Jong, M. V. Zijverden, A. N. J. A. M. Sips and R. E. Geertsma, *Nanotoxicology*, 2009, **3(2)**, 109.

2 O. Bar-Ilan, R. M. Albrecht, V. E. Fako and D. Y. Furgeson, *Small*, 2009, **5**, 1897.

3 M. L. Cohen, *Nature*, 2000, **406**, 762.

4 P. Fernandes, *Nat. Biotechnol.*, 2006, **24**, 1497.

5 J. Clardy, M. A. Fischbach and C. T. Walsh, *Nat. Biotechnol.*, 2006, **24**, 1541.

6 D. J. Payne, M. N. Gwynn, D. J. Holmes and D. L. Pompliano, *Nat. Rev. Drug Discov.*, 2007, **6**, 29.

7 L. L. Silver, *Nat. Rev. Drug Discov.*, 2007, **6**, 41.

8 D. Hopwood, S. Levy, R. P. Wenzel, N. Georgopapadakou, R. H. Baltz, S. Bhavnani and E. Cox, *Nat. Rev. Drug Discov.*, 2007, **6**, 8.

9 A. J. Huh and Y. J. Kwon, *J. Control. Release*, 2011, **156**, 128.

10 S. Mitragotri and J. Lahann, *Nat. Mater.*, 2009, **8**, 15.

11 B. Kowalczyk, K. J. M. Bishop, I. Lagzi, D. Wang, Y. Wei, S. Han and B. A. Grzybowski, *Nat. Mater.*, 2012, **11**, 227.

12 L. Li and H. Wang, *Adv. Healthcare Mater.*, 2013, **2**, 1351.

13 L. Liu, K. Xu, H. Wang, J. P. K. Tan, W. Fan, S. S. Venkatraman, L. Li and Y.-Y. Yang, *Nat. Nanotechnol.*, 2009, **4**, 457.

14 D. A. Salick, D. J. Pochan and J. P. Schneider, *Adv. Mater.*, 2009, **21**, 4120.

15 A. S. Veiga, C. Sinthuvanich, D. Gaspar, H. G. Franquelim, M. A. R. B. Castanho and J. P. Schneider, *Biomaterials*, 2012, **33**, 8907.

16 K. A. Brogden, *Nat. Rev. Microbiol.*, 2005, **3**, 238.

17 A. Schmidtchen, I. M. Frick, E. Andersson, H. Tapper and L. Bjorck, *Mol. Microbiol.*, 2002, **46**, 157.

18 T. Koprivnjak and A. Peschel, *Cell. Mol. Life Sci.*, 2011, **68**, 2243.

19 P. Gwynne, *Nature*, 2013, **495**, S12.

20 K. Weintraub, *Nature*, 2013, **495**, S14.

21 P. Ghosh, G. Han, M. De, C. K. Kim and V. M. Rotello, *Adv. Drug Deliv. Rev.*, 2008, **60**, 1307.

22 H. Ke, J. Wang, Z. Dai, Y. Jin, E. Qu, Z. Xing, C. Guo, X. Yue and J. Liu, *Angew. Chem. Int. Ed. Engl.*, 2011, **50**, 3017.
23 C. R. Patra, R. Bhattacharya, D. Mukhopadhyay and P. Mukherjee, *Adv. Drug Deliv. Rev.*, 2010, **62**, 346.
24 M. Vukomanović, S. D. Škapin and D. Suvorov, *Slo Pat. Appl.*, 201200204, 2012.
25 M. Quinet, F. Lallemand, L. Ricq, J.-Y. Hihn and P. Delobelle, *Surf. Coat. Tech.*, 2010, **204**, 3108.
26 M. P. Casaletto, A. Longo, A. Martorana, A. Prestianni and A. M. Venezia, *Surf. Interface Anal.*, 2006, **38**, 215.
27 D. Rautaray, S. Mandal and M. Sastry, *Langmuir*, 2005, **21**, 5185.
28 J. A. Scholl, A. L. Koh and J. A. Dionne, *Nature*, 2012, **483**, 421.
29 M. Vukomanović, I. Bračko, I. Poljanšek, D. Uskoković, S. D. Škapin, D. Suvorov, *Cryst. Growth Des.*, 2011, **11**, 3802.
30 M. Ericsson, D. Hanstorp, P. Hagberg, J. Enger and T. Nyström, *J. Bacteriol.*, 2000, **182**, 5551.
31 R. M. Donlan and J. W. Costerton, *Clin. Microbiol. Rev.*, 2002, **15**, 167.
32 W. He, X. Gu and S. Liu, *Adv. Funct. Mater.*, 2012, **22**, 4023.
33 D. Cui, A. Szarpak, I. Pignot-Paintrand, A. Varrot, T. Boudou, C. Detrembleur, C. Jérôme, C. Picart and R. Auzély-Velty, *Adv. Funct. Mater.*, 2010, **20**, 3303.

